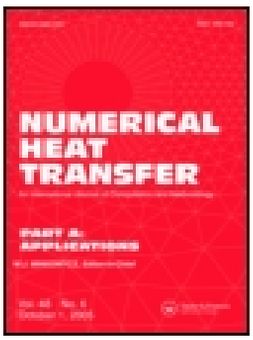

Numerical Heat Transfer, Part A: Applications

ISSN: 1040-7782 (Print) 1521-0634 (Online) Journal homepage: http://www.tandfonline.com/loi/unht20

NUMERICAL SIMULATION OF SOLUTE REDISTRIBUTION DURING TRANSIENT LIQUID PHASE BONDING PROCESS FOR AL-CU ALLOY

Tien-Chien Jen, Yuning Jiao

To cite this article: Tien-Chien Jen, Yuning Jiao (2001) NUMERICAL SIMULATION OF SOLUTE REDISTRIBUTION DURING TRANSIENT LIQUID PHASE BONDING PROCESS FOR AL-CU ALLOY, Numerical Heat Transfer, Part A: Applications, 39:2, 123-138, DOI: 10.1080/10407780119640

To link to this article: http://dx.doi.org/10.1080/10407780119640

Published online: 29 Oct 2010.

Submit your article to this journal

Article views: 21

View related articles

Citing articles: 1 View citing articles

Full Terms & Conditions of access and use can be found at
http://www.tandfonline.com/action/journalInformation?journalCode=unht20

Download by: [University of Johannesburg] **Date:** 24 September 2015, At: 03:24

Numerical Heat Transfer, Part A, 39:123–138, 2001
Copyright © 2001 Taylor & Francis
1040-7782/01 $12.00 + .00

Downloaded by [University of Johannesburg] at 03:24 24 September 2015

NUMERICAL SIMULATION OF SOLUTE REDISTRIBUTION DURING TRANSIENT LIQUID PHASE BONDING PROCESS FOR AL-CU ALLOY

Tien-Chien Jen and Yuning Jiao
Mechanical Engineering Department, University of Wisconsin, Milwaukee, Wisconsin 53211, USA.

A one-dimensional mathematical model is developed to predict the solute redistribution during the transient liquid phase (TLP) bonding process for Al-Cu alloy. The macroscopic solute diffusion in the liquid and the solid as well as for the solid transformation to the liquid because of the solute macrosegregation are considered in this study. The effects of holding temperatures and the interlayer thickness on the holding time, remelting layer thickness, and the mush zone thickness of the TLP bonding process are investigated. It is shown numerically that the holding time, the holding temperature, and the interlayer thickness influence the solute distribution strongly, which in turn influence the mush zone thickness significantly.

INTRODUCTION

Among many bonding techniques, the TLP process is unique in the sense of producing similar or even the same microstructure within the bonding interface. It is well known that in commercial welding technology the microstructure and crystal growth direction are changed because of the nonuniform heating and cooling processes involved [1]. This usually gives rise to lower bonding strength, in particular in a high temperature environment. Because of the solid and liquid state diffusion, film molten zone, and explicit crystal growth during the TLP process, single crystal growth is possible [2–5]. The motivation of this study is to develop a technology that enables bonding of two single crystal bulk materials with the maximum possible bonding strength using the TLP process technique. Note that this is particularly important to the applications such as the turbine blade system in the aerospace industry [6].

The principle of the TLP technique is to bond two crystals using an interlayer alloy. The melting temperature of the interlayer alloy should be less than the substrate (master) alloy. The isothermal heat treatment temperature is determined to be above 30–50°C of the melting point of the interlayer materials. After isothermal heat treatment, the interlayer is remelted and the liquid is filled fully with the two interfaces of the single crystals. The composition of bonds will reach equilibrium composition and move along the tie line. Thus, the solidification tem-

Received 11 August 2000; accepted 21 September 2000.
Address correspondence to T.-C. Jen, Mechanical Engineering Department, University of Wisconsin, Milwaukee, WI 53211, USA.

NOMENCLATURE

C	solute concentration	θ	dimensionless holding temperature
D	effective solute diffusivity	ρ	density
g	volume fraction of liquid or solid	τ	dimensionless time
j_c	solute diffusive flux		
L	interlayer thickness	**Subscripts**	
m	slope of the liquidus	Al	pure aluminum
t	time	I	interlayer
T	holding temperature	IO	initial condition of interlayer
T_L	liquidus temperature	l	liquid phase
T_M	melting point of the pure solvent	LI	interlayer in liquid state
T_S	solidus temperature	LM	master alloy in liquid state
U_l	superficial liquid velocity	M	master alloy
x	spatial coordinate perpendicular to the solid–liquid interface	MO	initial condition of master alloy
		s	solid phase
X	dimensionless x-coordinate	SI	interlayer in solid state
ϕ	dimensionless concentration	SM	master alloy in solid state

Downloaded by [University of Johannesburg] at 03:24 24 September 2015

perature increases and the volume of liquid decreases. The growth is similar to that of laser remelted metals, epitaxial growth based on the base materials. Finally, after sufficient isothermal heat treatment, the liquids disappear and bond the two single crystals into one single crystal without the formation of a recrystallized zone at the bonds if the two single crystals have the same orientation.

TLP bonding has been developed to join the superalloys susceptible to hot cracking [3]. It is very important to design a suitable interlayer alloy that does not contain any deleterious phases and has a melting point lower than that of the base metal [7, 8, 11, 12]. Now the interlayer alloys that generally are used for superalloys are of the Ni-Cr-Si-B system. However, the addition of Si and B should be avoided because these elements are harmful impurity elements in single crystal superalloys. Hafnium (Hf) is a beneficial element for improving the intermediate temperature creep properties and strengthening the $\grave{\gamma}$ phase [9]. Thus, the interlayer containing Hf was developed for bonding the DD3 Ni-based single crystal, and the $\gamma/\grave{\gamma}$ two-phase structure was obtained in the bonding layer [10]. However, the interlayer containing Hf was developed for the first-generation Ni-based superalloys that are free-Re superalloys. Until now, there has been no investigation of the interlayer materials TLP bonding for Re-containing Ni-based superalloys. Therefore, it is necessary to develop a new interlayer with high properties to maintain the strength of the bond and keep the strength equivalent to that of the base alloy.

So far, almost all the earlier work concentrated on the microstructure research. Zheng et al. [4] improved the TLP process to bond two Ni-based single crystals without a second phase existing in the bonds. They solved this problem by developing an interlayer containing Hf without B and Si. They found the melting temperature of Ni_5H_f is 1130–1160°C and the maximum solubility of Hf in $\grave{\gamma}$

can reach 7 at%. Ohashi et al. [13] investigated the relationship between the disorientation angle at the bonding interface and joint strength. Guan and Gale [10] and Gale et al. [11] presented an investigation of transient liquid phase bonding of a single crystal NiAl to a conventional polycrystalline Ni-based superalloy MM247. They proposed a wide-gap TLP bonding process in their study. In wide-gap TLP bonding, a composite interlayer consisting of a liquid forming matrix, plus a (nominally) nonmelting constituent, is employed.

Accurate control of the crystal growth of bonding two bulk single crystals using the TLP process is crucial to improving product quality, in particular for the turbine blade system, for example, used the aerospace industry. Computer simulation in the remelting and solidification processes is useful to predict the microstructure, crystal orientation, and mechanical properties under the TLP process. However, so far, numerical simulation has been used rarely in the development of the bonding of single crystal alloys especially using the TLP process. The primary objective of this study is to develop the mathematical model of the solute diffusion that can be used for the TLP process for Al-Cu alloy. The macroscopic solute diffusion in the liquid and the solid as well as for the solid transformation to the liquid because of the solute macrosegregation are considered in this study. The effects of holding temperatures and the interlayer thickness on the holding time, remelting layer thickness, and the mush zone thickness of the TLP bonding process are investigated.

Downloaded by [University of Johannesburg] at 03:24 24 September 2015

THEORETICAL ANALYSIS

Consider two master single crystal alloys to be joined with an interlayer in between as shown in Figure 1. It is assumed that the thermal properties and mass diffusivities are constant, and the entire system is exposed to a constant holding temperature when the system instantaneously reaches this temperature. Typically, the interlayer is about 30–50°C lower than the master alloys' melting temperature. Thus, it is important to choose the appropriate holding temperature that should be in between the melting temperature of the interlayer and the master alloy. As shown in Figure 1, a liquid interlayer is formed in between two master alloys during initial heat treatment. As holding time increases, because of the mass diffusion into the master alloy, the melting temperature deceases near the interlayer. Thus, a remelting layer was formed and the interface moves into the master alloy. Note that the thickness of this remelting layer is critical in determining the bonding strength of the TLP process. Also, a mushy zone is generated because of solute redistribution in the master alloy; this causes the coexistence of liquid and solid phases. Note that the formation of the mush zone may be detrimental to the single crystal growth and consequently decreases the strength of the bonding layer strength.

Mathematical Formulation

The model based on the Fick's law, including the effect of solid remelting, is used in this study. Adding the volume conservation equations within the solid and liquid phases, we obtain the following macroscopic conservation equation

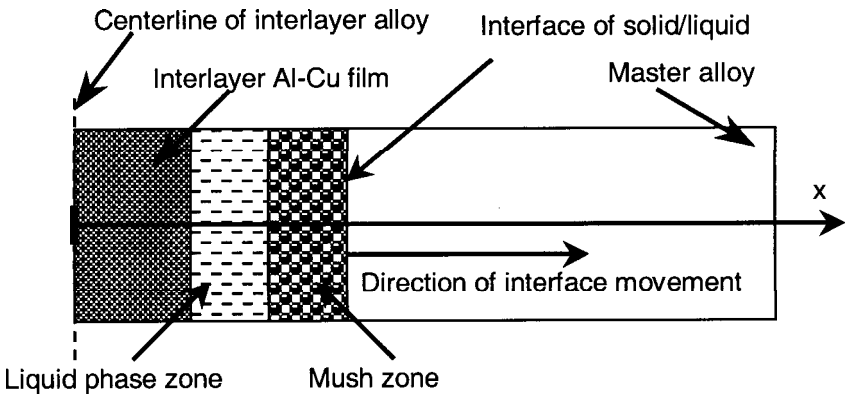

Figure 1. Schematic representation of the physical domain.

Downloaded by [University of Johannesburg] at 03:24 24 September 2015

for the solute concentration [14]:

$$\frac{\partial(\rho_{l,s}C_{l,s})}{\partial t}+\frac{\partial(\rho_{l,s}C_{l,s}U_l)}{\partial x}=-\frac{\partial j_c}{\partial x} \tag{1}$$

where t, $\rho_{l,s}$, $C_{l,s}$, U_l, and j_c are the time, liquid or solid density, liquid or solid solute concentration, superficial liquid velocity, and solute diffusive flux, respectively. Assuming the solid phase is stationary and the dispersion flux is negligible, we can model the diffusive solute flux as follows:

$$j_c=-g_{l,s}\rho_{l,s}D_{ls}\frac{\partial C_{l,s}}{\partial x} \tag{2}$$

where $g_{l,s}$ is the volume fraction of the liquid or solid and $D_{l,s}$ is the effective solute diffusivity in the liquid or solid. When the mushy zone is small, we have $g_{l,s}=1$. Thus, Eq. (2) can be modeled as follows:

$$j_c=-\rho_{l,s}D_{l,s}\frac{\partial C_{l,s}}{\partial x} \tag{3}$$

Assuming that we have the thermodynamic equilibrium at the solid–liquid interface and a uniform concentration locally in the liquid, the liquid concentration can be related to the temperature by the liquidus of the phase diagram as follows:

$$C_l=(T-T_M)/m \tag{4}$$

where, T_M is the melting point of the pure solvent and m is the slope of the liquidus.

The interlayer and master alloy are assumed to be initially at uniform solute concentration:

$$C_I=C_{I0} \quad \text{at } 0<x<L/2 \quad t=0 \tag{5}$$

$$C_M=C_{M0} \quad \text{at } x>L/2 \quad t=0 \tag{6}$$

The boundary conditions in the TLP process are as follows:

The solute concentration far from the interlayer is assumed to remain at the initial concentration C_{M0}:

$$C_M = C_{M0} \quad \text{at } x = \infty \tag{7}$$

At the interlayer centerline, the concentration flux can be obtained from the symmetric distribution of the solute concentration:

$$\left.\frac{\partial C_l}{\partial x}\right|_{x=0} = 0 \tag{8}$$

The equations listed above can be nondimensionalized with the interlayer thickness L as the characteristic length, L^2/D_{LI} as the characteristic time, and C_0 as the characteristic solute concentration. The following dimensionless distance X, time τ, concentration ϕ, and holding temperature θ can be defined as

$$X = \frac{x}{L} \quad \tau = \frac{tD_{LI}}{L^2} \quad \phi = \frac{C}{C_{I0}} \quad \theta = \frac{T - T_M}{mC_0} \tag{9}$$

All the equations listed above then can be nondimensionlized as follows:

For the liquid region in the interlayer (LI),

$$\frac{\partial \phi_{LI}}{\partial \tau} = \frac{\partial^2 \phi_{LI}}{\partial X^2} \tag{10}$$

For the solid region in the interlayer (SI),

$$\frac{\partial \phi_{SI}}{\partial \tau} = \frac{\partial}{\partial X}\left(\frac{D_{SI}}{D_{LI}}\frac{\partial \phi_{SI}}{\partial X}\right) \tag{11}$$

For the liquid region in the master alloy (LM),

$$\frac{\partial \phi_{LM}}{\partial \tau} = \frac{\partial}{\partial X}\left(\frac{D_{LM}}{D_{LI}}\frac{\partial \phi_{LM}}{\partial X}\right) \tag{12}$$

and for the solid region in the master alloy (SM),

$$\frac{\partial \phi_{SM}}{\partial \tau} = \frac{\partial}{\partial X}\left(\frac{D_{SM}}{D_{LI}}\frac{\partial \phi_{SM}}{\partial X}\right) \tag{13}$$

The dimensionless form of Eq. (4) can be obtained by

$$\phi_{(S,L)M} = \theta \tag{14}$$

The nondimensional initial conditions for the solute concentration in the interlayer and master alloy can be given, respectively,

$$\phi_I = \phi_{10} \quad \text{at } 0 < X < \tfrac{1}{2} \quad \tau = 0 \tag{15}$$

$$\phi_M = \phi_{M0} \quad \text{at } X > \tfrac{1}{2} \quad \tau = 0 \tag{16}$$

The nondimensional boundary conditions are as follows:

$$\phi_M = \phi_{M0} \quad \text{at } X = \infty \tag{17}$$

$$\left.\frac{\partial \phi_M}{\partial X}\right|_{X=0} = 0 \tag{18}$$

It can be seen from the dimensional analysis that four sets of dimensionless par-

Downloaded by [University of Johannesburg] at 03:24 24 September 2015

ameters are generated; they are D_{SI}/D_{LI}, D_{LM}/D_{LI}, D_{SM}/D_{LI}, and θ. The first three parameters are the mass diffusivity ratio between the solid solute and the liquid solute in the master alloy and interlayer. The last parameter is dependent on the holding temperature and the material physical properties. In general, the effective mass diffusivities of the liquid solute (i.e., D_{LI} and D_{LM}) can be assumed to be identical, and the same assumption can be made for the effective mass diffusivities of the solid solute (i.e., D_{SI} and D_{SM}). With these assumptions, the parameters are now reduced to only two; they are D_{SI}/D_{LI} and θ. Physically, the first parameter denotes the relative mass diffusion penetration capabilities of the liquid solute versus the solid solute. The larger the ratio, the faster the solute concentration penetrates further into the mass alloy. The second parameter is the dimensionless holding temperature. In this study, we will limit our investigation to the effect of the second parameter, holding temperatures, to the solute redistribution in the interlayer and master alloy for Al-Cu (4.5% wt) alloy.

Downloaded by [University of Johannesburg] at 03:24 24 September 2015

Numerical Method and Grid Convergence Tests

The governing equations are solved numerically by the explicit finite volume method [16]. When we calculate, we assume that the solute diffusion coefficient in solid or liquid is the same; that means $D_{LI} = D_{LM}$, $D_{SI} = D_{SM}$. The computational domain is chosen in such a way that it is large enough (i.e., from 3000 μm to 10,000 μm) to ensure the penetration depth is small enough in comparison to the total computational domain. The effective solute diffusivity in the liquid or solid master Al-Cu alloy, D_{LM} and D_{SM}, are 0.0035 mm^2/s and 0.0001 mm^2/s, respectively [15]. The Al-Cu alloy phase diagram is shown in Figure 2. Note that to calculate the liquidus and solidus temperature for the solute, linear regressions for both curves are used:

$$\textbf{Liquidus :} \quad T_L = T_{Al} - m_L \times C_{Al} \tag{19}$$

$$\textbf{Solidus :} \quad T_S = T_{Al} - m_S \times C_{Al} \tag{20}$$

where T_L, T_S, and T_{Al} denote liquidus, solidus, and pure aluminum melting temperatures, respectively. m_L and m_S are the slopes of the liquidus and solidus curves in the phase diagram, and C_{Al} is the solute concentration (in wt%). Note that for the Al-Cu alloy, the $T_{Al} = 660.452^{\circ}C$, $m_L = 3.52$, and $m_S = 18.71$ (see Figure 2).

To ensure the grid size and time step are small enough for the convergence of the solution, detailed grid convergence tests have been performed as shown in Table 1. It can be seen from the table that when the grid size changes from 0.05 μm to 0.5 μm and the time step varies from 0.05 sec to 1 sec, the numerical error is less than 3.7%. Thus, a grid size of $\Delta x = 0.5$ μm and a time step of $\Delta t = 1$ sec are used throughout this study to ensure the grid independence. This model is verified further by comparing the numerical results presented by Havard and Asbjorn [15] for the solute redistribution of Al-4.5wt% C_u alloy in the unidirectional solidification without the effect of remelting. The agreements between the current model and Havard and Asbjorn's results were found to be very good (not shown). With this agreement and the grid convergence tests shown before, we are confident that this

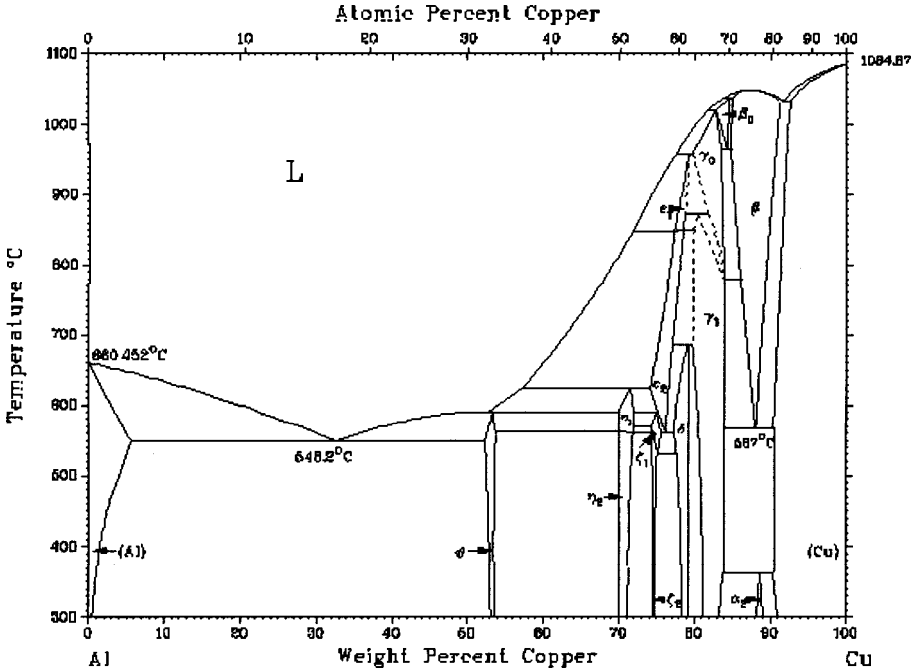

Figure 2. Al-Cu phase diagram.

numerical model is valid to further compute the solute redistribution during the TLP process.

RESULTS AND DISCUSSION

To quantify the effect of macroscale solute diffusion on the solid–liquid interface movement, remelting layer thickness, and mush zone thickness, the solute concentration distributions in the interlayer and master alloy are investigated. In this study, a one-dimensional model has been modified to account for the macroscopic solute diffusion in the liquid and the solid as well as for the solid transformation to the liquid because of the solute macrosegregation. The developed model is then applied to an Al-4.5% Cu interlayer alloy with two different interlayer

Table 1. Grid size and time step convergence tests

t, (sec)	1	1	1	0.05	0.1	0.5
Δx, (μm)	0.5	0.1	0.05	0.5	0.5	0.5
Maximum error of solute concentration from solid/liquid in master alloy	3.7%	2.2%	2.3%	1.3%	2.4%	1.6%

Downloaded by [University of Johannesburg] at 03:24 24 September 2015

thicknesses (i.e., 100 μm and 200 μm), and a pure Al master material is held at a given temperature. Since the melting temperature for the Al-Cu (4.5%wt) alloy in this study varies from 444.612°C to 660.452°C, four different holding temperatures, 645°C, 650°C, 655°C, and 660°C, unless otherwise stated, are chosen in this study.

The Solute Redistribution from the Interface

Figure 3 demonstrates the solute spatial concentration distribution for Al-Cu alloy at four different holding temperatures, 645°C, 650°C, 655°C, and 660°C, and three different times, 10, 40, and 100 hours. In this figure, the interlayer thickness used is 100 μm. It can be seen from the figure that the solute concentration decreases as the holding temperature increases. This is because the higher holding temperature leads to a larger liquid state solute region, which has a higher effective solute mass diffusitivity (i.e., $D_L \gg D_S$). This effect is more pronounced at larger times (i.e., for time larger than 40 hours) as shown in the figure. The solute concentration decreases as the time increases in the region $X < 200$ μm where very significant mass penetration occurs, and for $X > 200$ μm, the solute concentration increases as time increases. This causes the remelting of the master alloy in the short time when the solute concentration in the master alloy exceeds the melting point concentration at the holding temperature. Similarly, resolidification occurs at a longer time when the solute concentration is below the solidus curve. All these phenomena will be discussed in detail later.

Downloaded by [University of Johannesburg] at 03:24 24 September 2015

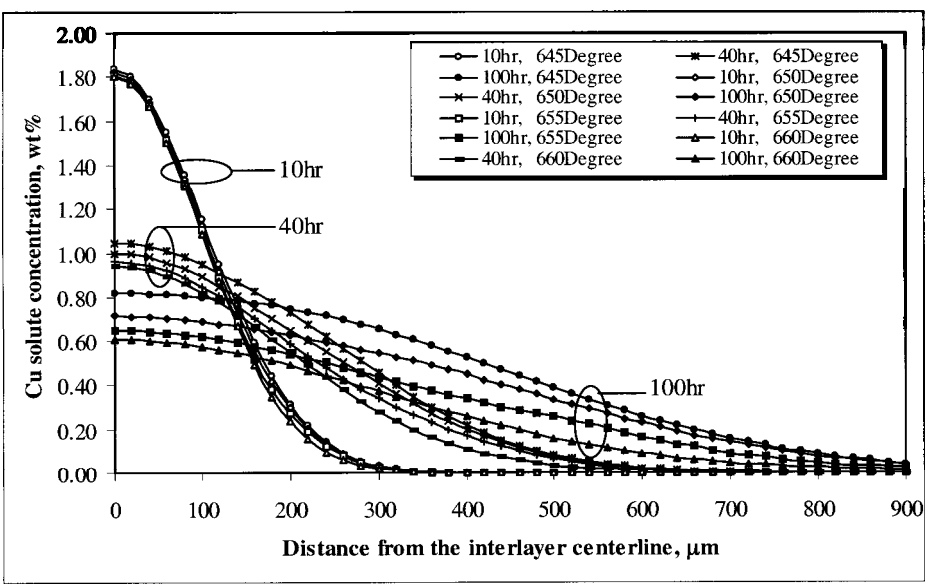

Figure 3. The solute spatial concentration distribution for Al-Cu alloy at different holding temperatures and different holding times.

Figure 4 depicts the temporal solute concentration distribution 5 μm into the master alloy and 5 μm into the Al-Cu interlayer from the interface at different holding temperatures. In a short transient time (i.e., less than 2 hours), the solute concentration decreases rapidly in the interlayer, and the reverse is true for the master alloy. Note that the solute concentration peaks at around 2 hours, which is when the Cu concentration reaches 2.0% wt in the master alloy; then solute concentration starts to decrease as the time increases. For the location 5 μm into the interlayer, the solute concentration first decreases rapidly in the first two hours until it reaches around 2.4% wt Cu concentration. After that, the decreasing rate slows down as shown in the figure. Note that in this early transient region, the holding temperatures do not have a strong influence on the solute concentration distribution. After this early transient region, the effect of the holding temperatures starts to set in. However, the solute concentration (at same holding temperature) difference at these two locations diminishes as time increases. After about 30 hours the solute concentrations at these two locations are essentially the same. The dominant factor driving the solute distribution after this time is the holding temperature (see Figure 4).

The solute concentration gradient at the liquid–solid interface is tracked and shown in Figure 5. It is worth pointing out that the concentration gradient at the solid–liquid interface is the driving force for the remelting and resolidification of the master alloy in the TLP process. It can be seen from this figure that at larger holding temperatures, the concentration gradient becomes smaller. This reveals that at a lower holding temperature the solute mass diffusion is stronger. Note that this

Downloaded by [University of Johannesburg] at 03:24 24 September 2015

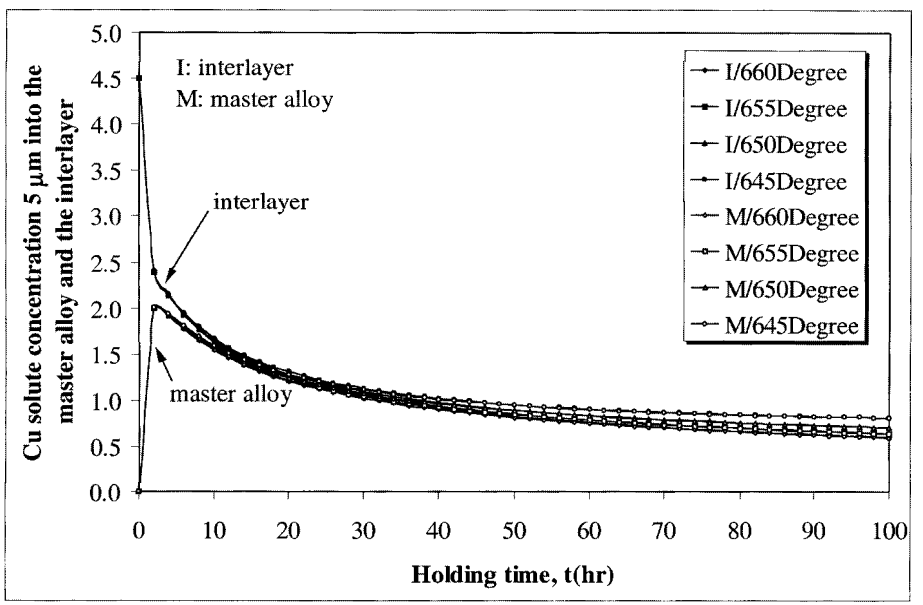

Figure 4. The temporal solute concentration distribution 5 μm into the master alloy and 5 μm into the Al-Cu interlayer from the interface at different holding temperatures.

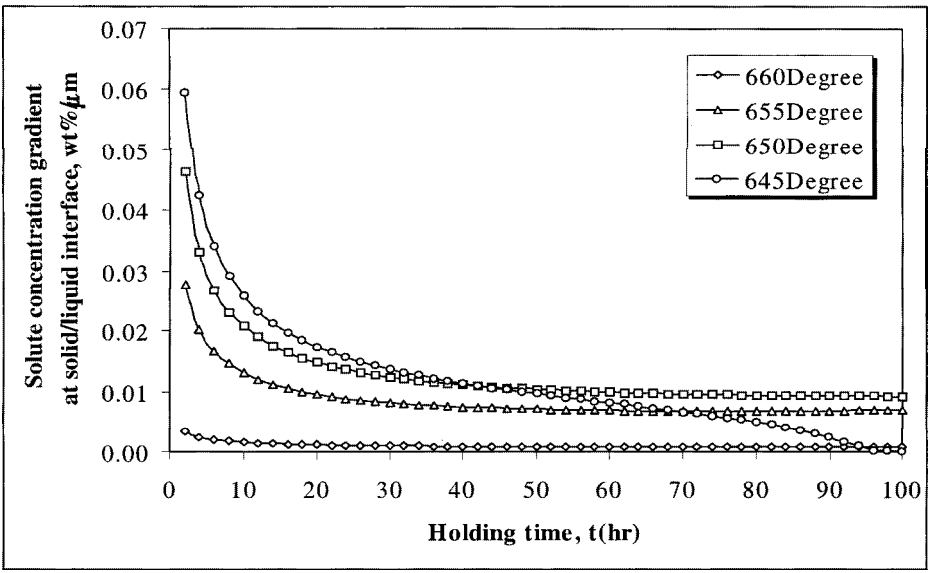

Figure 5. The solute concentration gradient at the liquid–solid interface.

does not mean that the concentration is lower for low holding temperatures, because a larger holding temperature has a larger liquid region, which has a higher effective solute diffusion coefficient (see Figure 3). An interesting phenomenon observed in this figure is that for the curve of the holding temperature at 645°C, the solute concentration gradient decreases significantly after about 40 hours and moves close to zero after 90 hours. This is because the resolidification phenomena occur when the solute concentration falls below 0.826% wt (see Figure 3). Table 2 shows the solute concentration intervals for different phase regions at various holding temperatures.

The effect of different interlayer thicknesses on the solute concentration distribution is demonstrated in Figure 6. Two different layer thicknesses are shown in this figure; they are 100 μm and 200 μm, and the holding temperature in this demonstration is set to be at 650°C. A strong effect on the solute concentration

Table 2. The solute concentration intervals for different phase regions at various holding temperatures

	Concentration (wt%), C		
Temperature (°C)	Liquid zone	Mush zone	Solid zone
645	$C > 4.39$	$0.826 < C < 4.39$	$C < 0.826$
650	$C > 2.97$	$0.559 < C < 2.97$	$C < 0.559$
655	$C > 1.55$	$0.291 < C < 1.55$	$C < 0.291$
660	$C > 0.128$	$0.024 < C < 0.128$	$C < 0.024$

Downloaded by [University of Johannesburg] at 03:24 24 September 2015

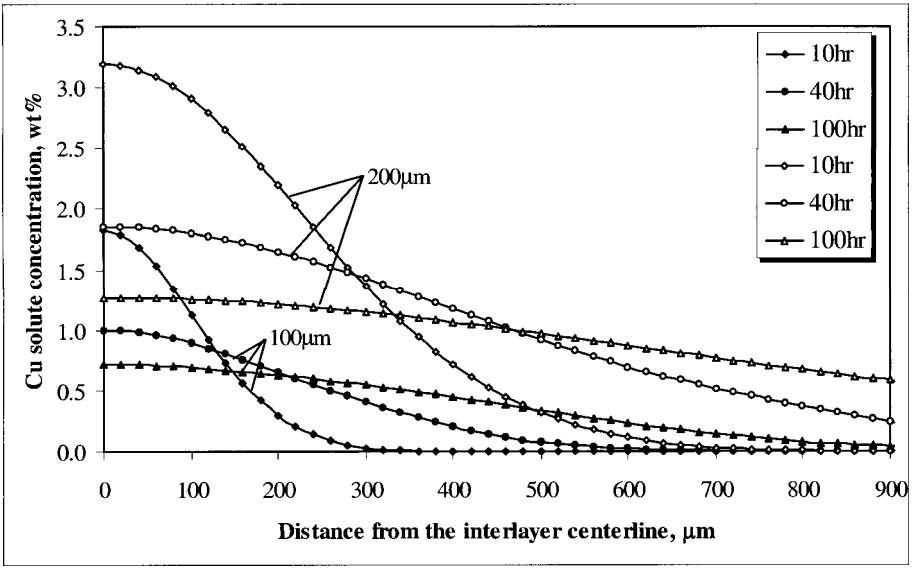

Figure 6. The effect of different interlayer thicknesses on the solute concentration distribution.

Downloaded by [University of Johannesburg] at 03:24 24 September 2015

distribution can be seen clearly in the figure. For the cases with 200 μm interlayer thickness, the solute concentration is about 80% higher than the cases with the 100 μm interlayer thickness, at the same time (i.e., 10, 40, or 100 hours). Also, the penetration depth for the former cases are much larger, which means larger master alloy thickness is required, and the time required for resolidication is much longer. Note that larger penetration depth also means a larger remelting layer, which may be favorable for better bonding strength, but the time for the bonding process may be prohibitively long.

The Effect of Solute Diffusion on the Solid–Liquid Interface Movement

As mentioned above, the solute diffusion causes the melting temperature to change in the interlayer and master alloy (see Table 1 and Eqs. (19) and (20)). Decreasing the solute concentration in the interlayer increases its melting temperature; while at the master alloy its melting temperature decreases because of increases in solute concentration. Thus where the master alloy is contiguous to the interlayer may be molten depending on the holding temperature applied. If the holding temperature is larger than the melting temperature adjacent to the interlayer, the master alloy will be molten; this results in the solid–liquid interface movement. Figure 7 indicates the solid–liquid interface movement at different holding temperatures and holding times for two different interlayer thicknesses. It can be seen that with the increase in the holding temperature, the solid–liquid interface

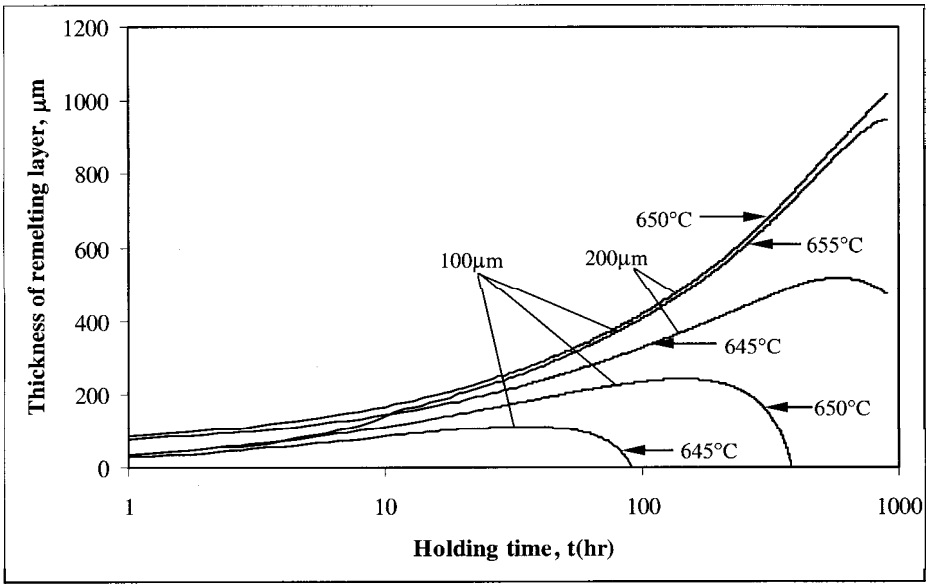

Figure 7. The solid–liquid interface movement at different holding temperatures and holding times for two different interlayer thicknesses.

Downloaded by [University of Johannesburg] at 03:24 24 September 2015

movement increases progressively with respect to time until it reaches a maximum. After this maximum is reached, the remelting layer starts to decreases, where the resolidification process begins. This will continue until all the material solidifies (for both interlayer and master alloy). This phenomenon is caused by the solute concentration redistribution as the mass concentration of Cu penetrates further into the master alloy. Note that the solute concentration in the interlayer decreases as the holding time increases, and the solute concentration of master alloy in the region near the interlayer increases early (see Figure 4). This causes the remelting layer to grow. However, as time progresses, the solute concentration deceases as the driving mass concentration in the interlayer falls below the liquidus concentration. Thus, at that point, the remelting layer starts to solidify. These can be seen clearly in the figure, for example, for the case with a 100 μm interlayer thickness at a holding temperature of 645°C. In this curve, the remelting layer starts to grow until it reaches about 25 hours holding time, where the maximum remelting layer thickness is reached. After this holding time, it starts to solidify, and the complete remelting layer disappears at around 90 hours holding time. For the cases with 200 μm interlayer thickness, the time required for resolidification to begin is much longer for the 100 μm interlayer thickness cases. For example, the resolidification starts at around 150 holding hours for the 100 μm case with holding temperature at 650°C, whereas under the same holding temperature for the 200 μm case, the time increases to more than 900 hours. However, as mentioned earlier, the remelting layer is larger for the latter case, which may result in better bonding strength.

Figure 8 shows the maximum remelting thickness and the holding time to achieve this thickness with respect to the holding temperatures. This is for the case with 100 μm interlayer thickness of Al-Cu alloy. It can be seen from the figure that the maximum remelting layer thickness increases with the holding temperature, and the time required to achieve this thickness also increases with the holding temperature. Note that it is desirable to have a larger remelting layer (stronger bonding) and shorter holding time (less energy consumption). However, as can be seen from the figure, it is virtually impossible to achieve both goals; instead judgment must be used to choose the preferred conditions to obtain the most economical solution.

Downloaded by [University of Johannesburg] at 03:24 24 September 2015

The Thickness of Mush Zone in Master Material

Figure 9 depicts the effect of the holding temperature and time on the thickness of the mush zone in the master alloy material. Note that the mush zone thickness is critical for the single crystal growth in the master alloy. In general, the mush zone is detrimental to the formation of a single crystal alloy and thus should be either avoided or eliminated in some way to optimize the strength of the bonding. In this figure, it can be seen that almost all the remelting layers are much zones for low holding temperatures, e.g., 645°C and 650°C. This can be explained easily: The lower holding temperature means a larger two-phase zone (i.e., where liquid and solid coexist) in the remelting layer (see Figure 2 and Table 2). This reveals that essentially there is no pure liquid phase in the TLP processes under such holding temperatures.

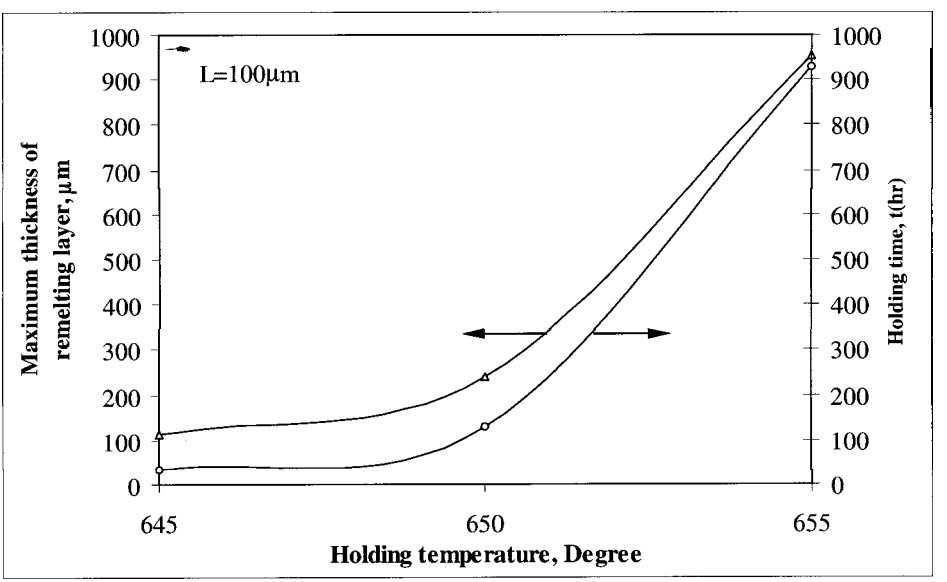

Figure 8. The maximum remelting thickness and the holding time to achieve this thickness with respect to the holding temperatures.

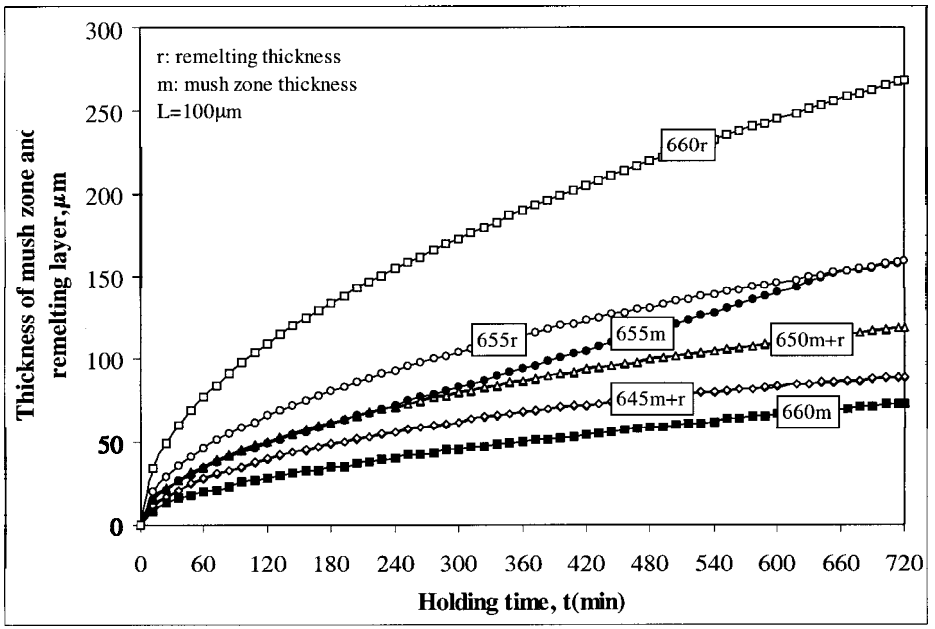

Figure 9. The effect of the holding temperature and time on the thickness of mush zone in master alloy material.

As the temperature increases to 655°C, there exists a pure liquid layer until the holding time exceeds 660 minutes. The difference between solid circular symbols and empty circular symbols is the thickness of the liquid phase layer. At this holding temperature, the much zone is still the dominant region in the remelting layer. When the temperature further increases to 660°C, a great portion of the remelting layer becomes the pure liquid phase. The pure liquid phase layer is about 3.5 times larger than the mush zone layer at this holding temperature. Again, this is because the holding temperature approaches the melting temperature of pure aluminum, where the two-phase region is very small at this holding temperature (see Figure 2 and Table 2). From the design point of view for single crystal bonding, the holding temperature should be as close to the pure aluminum temperature as possible, since the pure liquid phase layer is the largest. This is favorable since a single crystal can be regrown from the single crystal master alloy.

CONCLUSIONS

A one-dimensional mathematical model is developed to predict the solute redistribution during the TLP bonding process for Al-Cu alloy. The macroscopic solute diffusion in the liquid and the solid as well as for the solid transformation to the liquid from the solute macrosegregation are considered in this study. The effects of holding temperatures and the interlayer thickness on the holding time,

Downloaded by [University of Johannesburg] at 03:24 24 September 2015

remelting layer thickness, and the mush zone thickness of the TLP bonding process are investigated. Several major conclusions from this study can be drawn as follows:

- The solute concentration decreases as the holding temperature increases. Near the interlayer, the solute concentration decreases as time increases, whereas away from the interlayer, the solute concentration increases with time.
- The solute concentration gradient increases as the holding temperature increases at the solid–liquid interface. This reveals that the resolidification process is slower for higher a holding temperature, which leads to a much longer TLP processing time.
- The larger the interlayer thickness, the larger the solute concentration at the same holding time. This may lead to a longer holding time.
- The thickness of the remelting layer increases with the holding temperatures as well as the holding time.
- In general, the thickness of the mush zone increases with the holding time. At lower holding temperatures, the mush zone occupies a great portion of the remelting layer. When the holding temperature approaches the pure aluminum temperature, the pure liquid layer becomes the dominant layer in the remelting layer.
- The optimal technique parameters for the TLP process are high holding temperature, long holding time, and small interlayer thickness, because the pure liquid phase layer, which is favorable for single-crystal growth, is the largest in this case.

Downloaded by [University of Johannesburg] at 03:24 24 September 2015

REFERENCES

1. S. F. Milton Lima, P. Gilgien, and W. Kurz, Microstructure Selection in Laser Remelted Fe-C-Si Alloys, *Z. Metallkd*, vol. 89, no. 11, pp 751–757, 1998.
2. W. F. Gale and Z. A. M. Abdo, Bulk Alloy Micro-Structural Analogues for Transient Liquid Phase Bonds in the NiAl/Cu/Ni System, *Metall. Mater. Trans.* A, vol 30, no. 12, pp. 3111–3124, 1999.
3. E. F. Bradley, Superalloys and their application, in *Superalloys—A Technical Guide*, ASM International, Metals Park, OH, pp. 22–28, 1988.
4. Y. Zheng, R. Wang, and C. Li, *Proceeding of the First ASM European and Techniques for Structure Application*, Paris, France, pp. 111–116, 1987.
5. Z. Ruan, S. Wang, and Y. Zheng, Microstructure and Bonding Behavior of a New Hf-Bearing Interlayer Alloy for Single Crystal Nickel-Base Superalloy, *Scri. Mat.*, vol. 34, pp. 163–168, 1996.
6. W. F. Gale and Y. Guan, Transient Liquid Phase Bonding of NiAl Intermetallic Compound to Nickel-Base Superalloys—A Microstructural Investigation, in *Proceedings of the Fifth International Conference on Trends in Welding Research*, ASM International, pp. 663–668, 1999.
7. W. F. Gale and E. R. Wallach, Influence of Isothermal Solidification on Microstructural Development with Ni-Si-B Filler Metals, *Mater. Sci. Technol.*, vol. 7, no. 12, pp. 1143–1148, 1991.
8. W. F. Gale and E. R. Wallach, Wetting of Nickel Alloys by Nickel Based Brazes, *Mater. Sci. Technol.*, vol. 6, no. 2, pp. 170–175, 1990.

9. W. F. Gale and Y. Guan, Wide-Gap Transient Liquid Phase Bonding of NiAl-Hf to a Nickel-Base Superalloy, *Mater. Sci. Technol.*, vol. 15, pp. 464–467, 1999.
10. Y. Guan and W. F. Gale, Transient Liquid Phase Bonding of a Hf-bearing Single-Crystal Nickel Aluminide to MM-247 Superalloy, *Master. Sci. Technol.* vol. 15, pp. 207–212, 1999.
11. W. F. Gale, T. C. Totemeier, and J. E. King, Transformation of Aluminide Intermetallic Coatings on Single Crystal Nickel-Base Superalloys During Heat Treatment and Subsequent Exposure, in *Proceedings of Heat and Surface '92*, Japan Technical Information Service, pp. 483–486, 1992.
12. W. F. Gale and E. R. Wallach, Wetting Mechanisms in High-Temperature Brazing of Nickel-Based Alloys, in *Recent Trends in Welding Science and Technology*, S. A. David and J. M. Vitek, eds., ASM, pp. 529–534, 1990.
13. O. Ohashi, S. Meguro, and T. Yamagata, Effect of Twist Angle on Mechanical Properties of Diffusion Bonded Joint Using Ni-Base Single Crystal Superalloy TMS-26, *Mat. Trans. JIM*, vol. 37, no. 9, pp. 1505–1510, 1996.
14. J. Ni and C. Beckermann, A Volume-Averaged Two-Phase Model for Solidification Transport Phenomena, *Metall. Trans. B*, vol. 22, pp. 349–361, 1991.
15. J. T. Havard and M. Asbjorn, The Effect of Macroscopic Solute Diffusion in the Liquid upon Surface Macrosegregation, *Metall. Trans. B*, vol. 28, pp. 665–669, 1997.
16. S. V. Patanker, *Numerical Heat Transfer and Fluid Flow*, Hemisphere, Washington, D.C. 1980.

Downloaded by [University of Johannesburg] at 03:24 24 September 2015